



This is a repository copy of *Durability and degradation mechanisms of GFRP reinforcement subjected to severe environments and sustained stress*.

White Rose Research Online URL for this paper:
<http://eprints.whiterose.ac.uk/132399/>

Version: Accepted Version

Article:

Fergani, H., Di Benedetti, M. orcid.org/0000-0001-7870-1323, Mias Oller, C. et al. (2 more authors) (2018) Durability and degradation mechanisms of GFRP reinforcement subjected to severe environments and sustained stress. *Construction and Building Materials*, 170. pp. 637-648. ISSN 0950-0618

<https://doi.org/10.1016/j.conbuildmat.2018.03.092>

Reuse

This article is distributed under the terms of the Creative Commons Attribution-NonCommercial-NoDerivs (CC BY-NC-ND) licence. This licence only allows you to download this work and share it with others as long as you credit the authors, but you can't change the article in any way or use it commercially. More information and the full terms of the licence here: <https://creativecommons.org/licenses/>

Takedown

If you consider content in White Rose Research Online to be in breach of UK law, please notify us by emailing eprints@whiterose.ac.uk including the URL of the record and the reason for the withdrawal request.



eprints@whiterose.ac.uk
<https://eprints.whiterose.ac.uk/>

1
2
3
4
5
6
7
8
9
10
11
12
13
14
15
16
17
18
19
20
21
22
23
24
25
26
27
28
29
30

Durability and degradation mechanisms of GFRP reinforcement subjected to severe environments and sustained stress

Hamed Fergani^{a,*}, Matteo Di Benedetti^a, Cristina Miàs Oller^b, Cyril Lynsdale^a, Maurizio Guadagnini^a

^a Department of Civil and Structural Engineering, University of Sheffield, Sheffield, S1 3JD, UK

^b Analysis and Advanced Materials for Structural Design (AMADE), University of Girona, Girona, Spain

Abstract

Despite the large amount of research that has been carried out to date on the use of glass fibre reinforced polymer (GFRP) bars in concrete, one factor still hindering their widespread use in civil engineering applications is the lack of comprehensive data on their long-term in-service performance. This paper presents the test results of an experimental study investigating the physical and mechanical properties of GFRP bars exposed to severe environments and subjected to different levels of sustained load. The test environments included moist concrete, alkaline solution and tap water, with temperatures varying from 20°C to 60°C. The mechanical properties of the bars were characterized through direct tension, flexural and inter-laminar shear tests, while the physical and chemical properties were determined through the implementation of a series of complementary techniques, including moisture absorption measurements, scanning electron microscope (SEM), Fourier Transform Infrared Spectroscopy (FTIR) and Energy dispersive x-ray analyses (EDX). The test results showed that the elevated temperatures play a key role in triggering and accelerating the development of critical degradation mechanisms. The reduction in the tensile strength of all conditioned samples subjected to a sustained stress equivalent to 3000 µε was always within the limits recommended in existing codes for high durability bars, while a lower average strength retention was observed for higher levels of sustained stress (equivalent to 5000 µε). Finally, it can be conclude that the long-term mechanical properties of the tested GFRP bars appeared to be mainly affected by moisture diffusion through the resin rich layer and debonding at the fibre/matrix interfaces due to the dissolution of the silane coupling agents.

Keywords

Environmental degradation; Fibre/matrix bond; Glass fibres; Mechanical properties; Microstructures

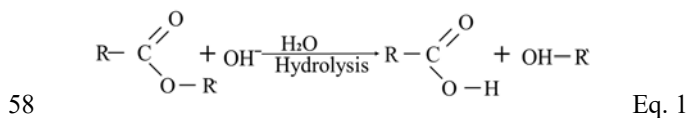
31 * Corresponding Author. Email address: hamed.fergani@sheffield.ac.uk

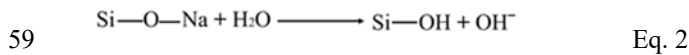
32 1 Introduction

33 Corrosion of steel reinforcement is one of the main causes of degradation of reinforced concrete (RC)
34 structures. In order to reduce the high maintenance cost associated with this problem, alternative reinforcing
35 materials, such as Fibre Reinforced Polymer (FRP) reinforcements, have been investigated over the past
36 three decades [1-4]. Despite the large amount of research that has been carried out on the use of FRP in
37 concrete, the lack of comprehensive data on their long-term in-service performance [3, 5] still hinders the
38 widespread use of FRP bars in civil engineering applications.

39 The durability of Glass FRP (GFRP) bars in concrete has usually been evaluated by using accelerated test
40 methods that expose the bars to environments harsher than those they may encounter in service and by
41 studying the change with time of their mechanical properties (i.e. tensile strength, bond strength and modulus
42 of elasticity) [2, 6-10]. In an attempt to achieve a more fundamental understanding of their long-term
43 behaviour, several researchers also investigated changes in physical, chemical and microstructural properties
44 using scanning electron microscopy (SEM) [4,11], energy dispersive x-ray analyses (EDX) [11,12], dynamic
45 mechanical analysis (DMA) [13], thermogravimetric analysis (TGA) [13,14], differential scanning
46 calorimetry (DSC) [10,14] and Fourier transform infrared spectroscopy (FTIR) [10,15].

47 Among the conditioning environments examined in the literature, moist and alkaline environments have been
48 reported to be the most detrimental for the GFRP matrix and the fibres [6, 16-19]. In particular, in moist
49 environments the free hydroxide ions (OH⁻) attack the polymer matrix and the long molecular chains are
50 disassembled by hydrolysis, promoting the ingress of more OH⁻ ions and water molecules (H₂O) (Eq. 1).
51 These, in turn, can break the polymer-polymer chain secondary bond, creating localized voids (increase in
52 free volume) and ultimately affecting the physical and mechanical properties of the GFRP matrix (i.e.
53 plasticization) [6]. The presence of water can also lead to the degradation of glass fibres through dissolution
54 (i.e. leaching) (Eq. 2). This process, which consists in the extraction of alkalis from the glass structures,
55 continues until alkalis are available. The hydroxide produced by the leaching process (Eq. 2) increases the
56 pH of the solution and, as the pH exceeds the threshold value of 9, the Si networks are affected (i.e., silica
57 dissolution in alkaline environment, Eq. 3). [19]





61 While direct submersion of bare bars in an alkaline and water solution at elevated temperature is
62 recommended by current standards to accelerate aging [20-22], previous studies [11, 18, 19] have shown that
63 these environments are excessively harsh and cause premature deterioration of GFRP bars, consequently lead
64 to conservative predictions of service life. As a result, researchers attempted to evaluate the performance of
65 GFRP bars by embedding them directly into concrete and exposing the specimens to high temperatures to
66 accelerate reaction rates, yet subjecting them only to the inherent alkaline and moist environment provided
67 by the concrete surrounding the bars [9,18,23].

68 In addition to the exposure environment, the presence of sustained stress might generate stress concentrations
69 around the micro-imperfections present in the matrix (e.g. pores) and accelerate the propagation of micro
70 cracks [24]. This, in turn, would ease the ingress of the surrounding media (e.g. alkali solution and water)
71 and have a possible detrimental impact on the durability of the fibres [25]. Only a limited number of studies
72 examined the influence of sustained stress on the long-term properties of FRP and concluded that low values
73 of sustained stress (20% of the ultimate strength or less) did not significantly affect the residual mechanical
74 properties. Such studies, however, only examined the performance of bare composite specimens [26], or
75 were limited to relatively low values of sustained stress (equivalent to a strain level of about 2000 $\mu\epsilon$) and did
76 not include any chemical/physical analysis of the microstructure [27].

77

78 **2 Research significance**

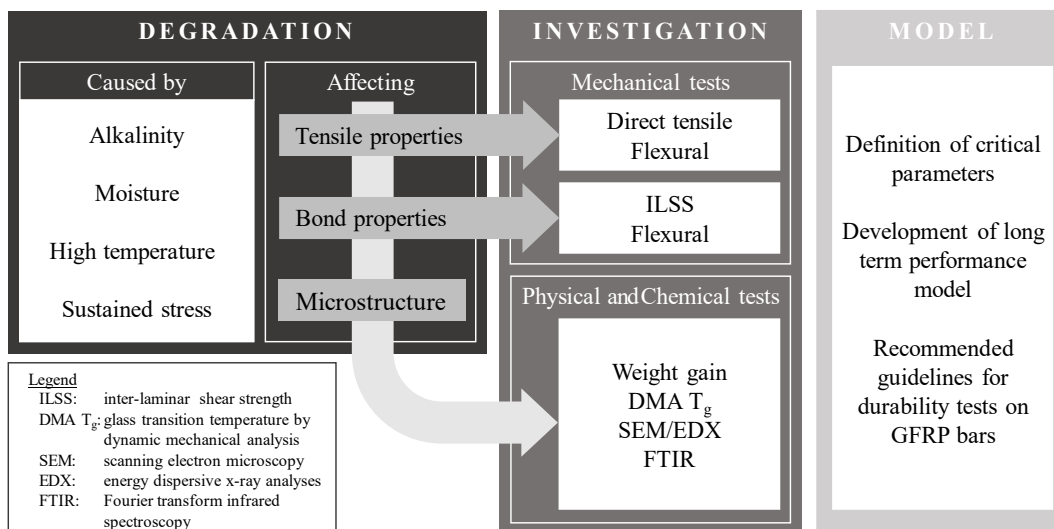
79 This study aims to provide a better understanding of the long-term performance of GFRP bars by employing
80 accelerated conditioning methodologies that more closely reflect the in-service conditions of GFRP RC
81 members including alkaline and moist environments as well as sustained stresses. A comprehensive
82 experimental programme was designed to study the degradation mechanisms at both micro (chemical
83 properties) and macro levels (physical and mechanical properties). Ultimately, the goal of this research is to
84 develop an effective model to assess and predict the durability of GFRP bars, which in turn, would directly
85 assist in the development of more reliable and less conservative design tools for GFRP RC members.

86

87 **3 Experimental programme**

88 **Fig. 1** presents a flow chart summarizing the complementary experimental program carried out in this
 89 research. The flow chart is divided in three sections: Section 1 – Degradation; Section 2 – Investigation; and
 90 Section 3 – Model. Section 1 shows the conditioning parameters (i.e. moist and alkali environments, high
 91 temperature and sustained stress) considered in this research and the GFRP bar properties that are affected (at
 92 both the macro level - tensile and bond properties - as well as at the micro level). Section 2 summarizes the
 93 tests used to assess the investigated material properties. The use of this complementary set of tests was
 94 implemented to enable a more comprehensive assessment of the degradation processes based not only on the
 95 outcomes of the mechanical tests but also on the results of the physical and chemical tests. Section 3 is
 96 presented in the chart as the logical convergence of this study, however a durability model still being
 97 developed and therefore will not be discussed in this paper.

98



99

100 **Fig. 1.** Overview of experimental program.

101 **3.1 Test Matrix**

102 The test matrix (Table 1) consisted of 334 GFRP samples obtained from bars with a nominal diameter of
 103 8mm. The GFRP bars used in this research work are commercially available and made of continuous E-
 104 CR Glass fibres impregnated with a vinyl ester resin and a glass fibre content of approximately 88% by
 105 weight. After the bars have gone through the pultrusion process, ribs are cut in the hardened bars and their
 106 surface is subsequently coated (**Fig. 2**).

107



108
109 **Fig. 2.** Appearance and surface geometry of the bar specimens

110 The program included tests on: unconditioned reference specimens (REF); unstressed and stressed bare bars
111 conditioned in alkaline solution (K and K-S3) or tap water (W and W-S3) at 20, 40 and 60°C; unstressed and
112 stressed bars embedded in concrete (i.e. moist and alkali environment) at ambient temperature (CON) and
113 immersed in tap water (M-CON, M-CON-S3 and M-CON-S5) at 20, 40 and 60°C. The exposure durations
114 taken into account varied from 1000 hr (~42 days) to 8760 hr (1 year).

115 Although it has been shown in previous research that direct exposure of GFRP to alkaline solution is
116 undoubtedly more aggressive than any realistic civil engineering application, such condition has been
117 included as it is recommended in current testing guidelines [21, 22]. The alkaline solution was prepared
118 according to the recommendations of the ACI 440 committee [22] using 118.5 g of Ca (OH)₂, 0.9 g of NaOH
119 and 4.2 g of KOH in 1 litre of deionised water. The pH level of this solution was periodically controlled and
120 kept at about 12.7, which is a representative value for a mature concrete pore solution [28].

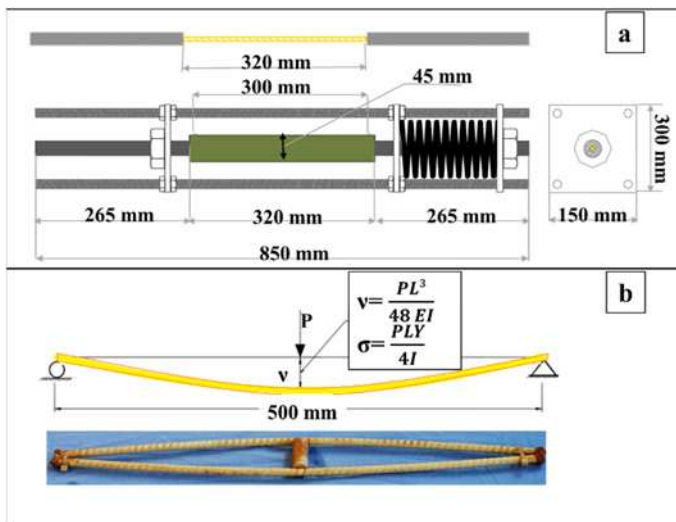
121 A sustained stress inducing a tensile strain of 3000 µε was applied to the FRP bars as recommended in ACI
122 440.3R and CAN/CSA-S806 [22,21], while a higher stress inducing a strain of 5000 µε was examined to
123 assess the effect of less stringent serviceability limits (corresponding to larger allowable crack widths and
124 deflections) [29]. The sustained stress inducing the desired level of tensile strain was applied using two
125 different configurations: via a spring of adequate stiffness mounted in a stiff pre-tensioning rig (**Fig. 2-a**); or
126 by tying pairs of specimens at the two ends with a wedge interposed at mid-length to impose the required
127 curvature (**Fig. 3-b**). During the conditioning period, the strain level of the bars was measured periodically
128 using a caliper and demec gauge system. The length of the steel springs used in the loading system were also
129 checked regularly using a digital caliper with an accuracy of 0.02 mm to assure that the load was maintained
130 constant.

131 Table 1 Test Matrix

Exposures	Conditioning		Test method						
	Temp (°C)	Time (hr)	MAb (N°)	TNS (N°)	ILSS (N°)	FLX (N°)	DMA (N°)	FTIR (N°)	SEM/EDX (N°)
REF	20	0		5	5	5	3	5	5

K	20	1000, 2000, 6480, 8760	3	9	3	3	1	3	2
	40		3	9	3	3	1	3	2
	60		3	9	3	3	1	3	2
K-S3	20	1000, 2000, 6480, 8760	4	9	3	3	N.A.	3	2
	40		4	9	3	3		3	2
	60		4	9	3	3		3	2
W	20	1000, 2000, 6480, 8760	3	N.A.	3	3	1	3	2
	40		3		3	3	1	3	2
	60		3		3	3	1	3	2
W-S3	20	1000, 2000, 6480, 8760	4	N.A.	3	3	N.A.	3	2
	40		4		3	3		3	2
	60		4		3	3		3	2
CON	20	2000, 6480, 8760	N.A.	9	N.A.	N.A.	N.A.	N.A.	N.A.
M-CON	20	1000, 2000, 6480	N.A.	9	N.A.	N.A.	N.A.	N.A.	N.A.
	40			9					
	60			9					
M-CON-S3	20	1000, 2000, 6480	N.A.	9	N.A.	N.A.	N.A.	N.A.	N.A.
	40			9					
	60			9					
M-CON-S5	60	42, 90, 270	N.A.	9	N.A.	N.A.	N.A.	N.A.	N.A.

132 Note: TNS, tensile test; MAb, water absorption test; ILSS, inter-laminar shear strength; FLX, flexural tests; DMA, T_g by
133 dynamic mechanical analysis; FTIR, Fourier transform infrared spectroscopy; SEM, scanning electron microscopy; EDX,
134 energy dispersive x-ray analyses; REF, reference samples; K, alkaline solution; W, tap water; M, moisture; CON, concrete;
135 S3 and S5 sustained stress at 3000 $\mu\epsilon$ and 5000 $\mu\epsilon$, respectively.
136



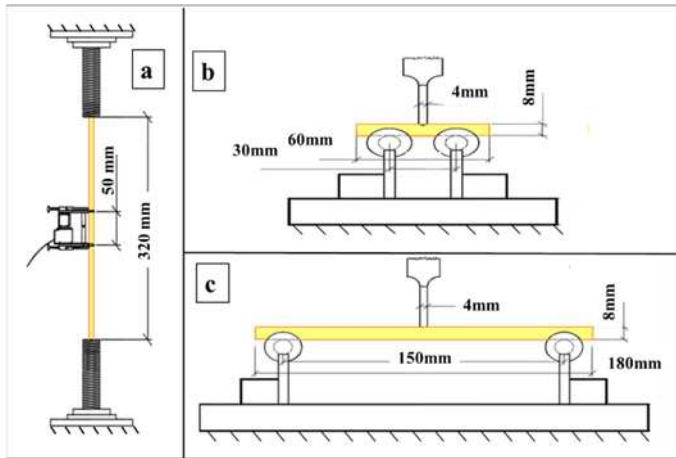
137
138 **Fig. 3.** Sketch illustrating the methods of application of sustained stress for (a) tensile and (b) moisture absorption test
139 specimens.
140

141 3.2 Test methodology

142 Direct tensile tests (TNS) [22], inter-laminar shear strength tests (ILSS) [30] and flexural tests (FLX) [31]
143 were carried out to evaluate the mechanical properties. All tests were performed in displacement control
144 using hydraulic and mechanical actuators with a maximum capacity of 1000 kN (TNS) and 10 kN (ILSS and

145 FLX), respectively. Data were recorded at 1 Hz using an NI LabVIEW data acquisition system. Details of the
146 setup of each test are shown in. **Fig. 4.**

147



148

149

150

Fig. 4. Set up for (a) tensile, (b) inter-laminar shear strength and (c) flexural tests.

151 A series of tests on the physical and chemical properties of the samples was also carried out to investigate the
152 microstructure and the integrity of the GFRP material before and after exposure. Standard test methods were
153 implemented to measure the glass transition temperature (T_g) by dynamic mechanical analysis (DMA) [32]
154 (**Fig. 5-a**) as well as moisture absorption (MAb) [33]. DMA was performed using a Mettler Toledo
155 DMA/SDTA861e machine while moisture absorption was assessed monthly by measuring the weight gain
156 due to fluid uptake into 300-mm-long (unstressed) and 450-mm-long (stressed) GFRP samples with the two
157 ends sealed using epoxy to prevent absorption from the cut edges. Prior to conditioning, the specimens were
158 dried in an oven at 55°C for 24 hr. The moisture uptake was monitored monthly using a digital scale with
159 accuracy of 0.001 g. For each set of measurements, the specimens were removed from their respective
160 conditioning environments at the same time, their surface was wiped dry with a cloth, and weighed
161 immediately. In addition, scanning electron microscopy (SEM), energy dispersive x-ray analyses (EDX) and
162 Fourier transforms infrared spectroscopy analysis (FTIR) were carried out following procedures available in
163 the literature [12, 34] (**Fig. 5-b**).

164

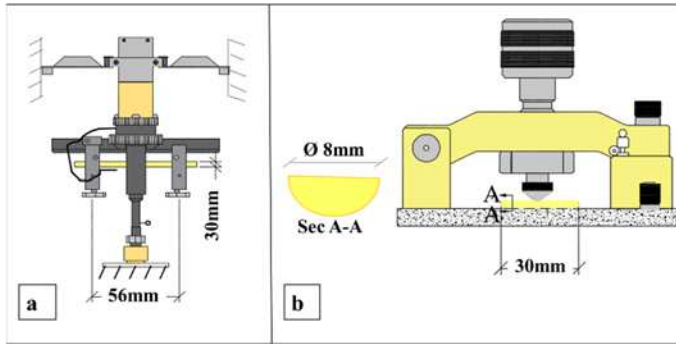


Fig. 5. Set up for (a) Tg and (b) FTIR tests.

165
 166
 167
 168 SEM and EDX were performed using a high magnification microscope (Phillips XL30 SEM) which uses a
 169 focussed scanned electron beam to produce images of the sample. Prior to the analysis, 10-mm-long samples
 170 were cut from the GFRP bars using a low speed diamond blade. The samples were subsequently placed
 171 vertically in moulds, cold-mounted in epoxy resin and cured for 24 hr at room temperature. The cross
 172 sections were then grinded using sand paper of increasing grit (400, 600, 800 and 1200) and polished with
 173 6 μm and 1 μm diamond pastes. The specimens were then carbon coated and analysed. Finally, FTIR
 174 analyses were performed using an FTIR spectrometer to investigate the external surface and the internal
 175 layers of the GFRP bars. In the former case, 30-mm-long samples were cut longitudinally from the bars up to
 176 a maximum depth of 3 mm, while in the latter the samples were prepared by grinding the GFRP bars into a
 177 fine powder (approximately 2 mg). The milled samples were pressed into a disc after being mixed with
 178 approximately 200 mg of anhydrous Potassium Bromide (KBr). The disc analysis was carried out by treating
 179 the KBr as the background reference. In both configurations, 32 scans were routinely obtained with an
 180 optical retardation of 0.25 cm to yield a resolution of 4 cm^{-1} . Typical characteristic absorption bands
 181 available in the literature are reported in **Error! Reference source not found.** Past studies on FRP
 182 examining civil engineering applications specifically focused on spectral zones in the band between 3600-
 183 2900 cm^{-1} including the stretching mode of the hydroxyl group OH (3450 cm^{-1}) and of the carbon-hydrogen
 184 group CH (2928 cm^{-1}) [12, 34]. In this research the acquisition of the spectra was performed ranging from
 185 4000 to 600 cm^{-1} , so as to include the stretching modes of C-O and C=C (1295 cm^{-1} and 920 cm^{-1}
 186 respectively).

187 Table 2 Assignments of the main absorption bands of the FTIR spectra

Absorption bands (cm^{-1})	Assignment
3400	O-H bending vibration
3026	C-H stretch of the benzene
2960, 2928, 2871	CH, CH ₂ , CH ₃ stretch
1722	C=O- Stretching vibration in saturated aldehyde, ketone or acid
1608, 1510	C=C- Stretching vibration of skeleton in benzene ring
1295	C-O stretch

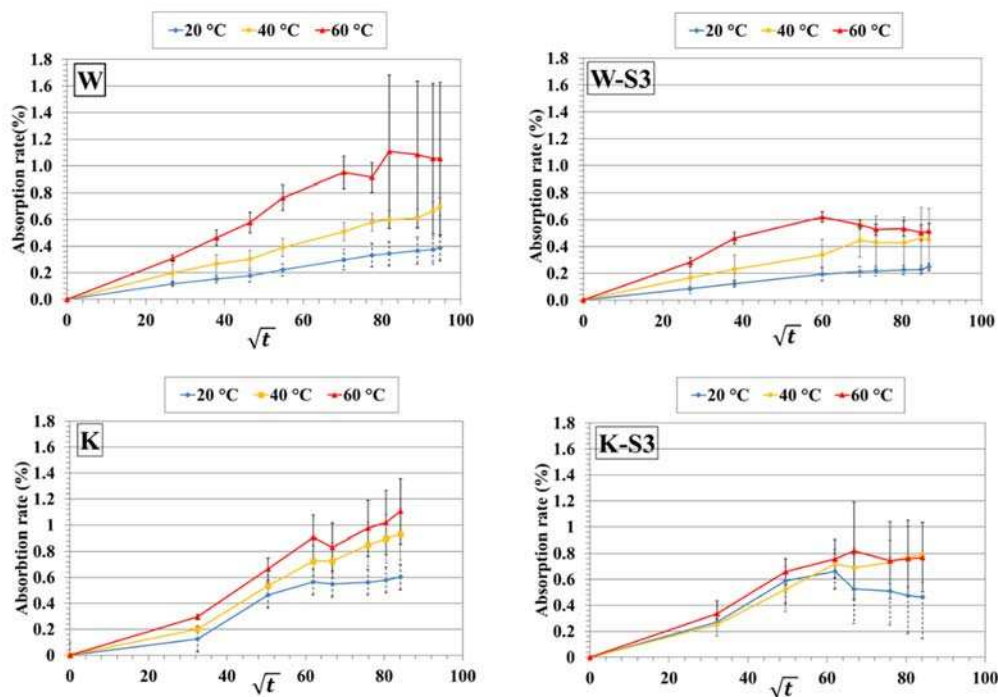
188

189 **4 Results and discussion**

190 The results of the experimental programme are presented in this section. Firstly, the results from the moisture
191 absorption tests, which can be used to investigate changes in the diffusion mechanism of water and alkaline
192 solutions, are reported and used to support the results of physical and chemical tests, which assessed the
193 deterioration of the micro structure (i.e., matrix, fibres and interface layer). Finally, the data acquired from all
194 tests is utilized to discuss the changes in mechanical properties at the macro scale.

195 **4.1 Moisture absorption properties**

196 **Fig. 6** shows the absorption rate of stressed (S3) and unstressed GFRP bars in water (W) and alkaline (K)
197 environment against the square root of the exposure time. The absorption rate was calculated as the ratio
198 between the average moisture uptake and the initial weight.



199

200 **Fig. 6.** Moisture absorption rate of unstressed and stressed (S3) GFRP bars immersed in water (W) and alkaline solution
201 (K) at different temperature.

202

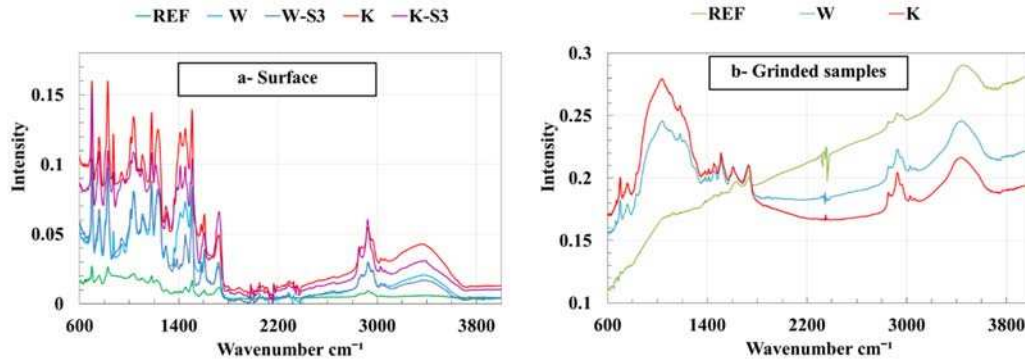
203 In all samples, weight increased gradually with respect to the exposure time, following the Fick's law up to
204 about 4500 hr ($\sim 67 \sqrt{\text{hr}}$). At this stage, the diffusion mechanism started to become unstable (non-Fickian
205 behaviour) resulting in absorption rate curves characterized by portions of weight loss, due to the degradation
206 of the outer layer leading to material loss, and by portions of weight gain, possibly due to the filling of new

207 or pre-existing voids and micro cracks. While no saturation was reached at the end of the considered ageing
208 period (8760 hr - $\sim 93 \sqrt{\text{hr}}$), stressed samples consistently showed a lower moisture uptake than unstressed
209 ones. This phenomenon could be attributed to the method used to stress the samples (i.e. bending, **Fig. 3b**)
210 which reduces the number of open pores in the portion of the bar in compression. This is discussed further in
211 section 4.2.2. In addition, the exposure temperature played a critical role on the absorption process. The
212 measured data showed that the higher the temperature the higher the absorption rate. This can be attributed to
213 an increase in the chemical reactions rate as well as to a higher void pressure resulting from an increase in
214 the volume of gases as temperature rises. This pressure build-up favoured the propagation of micro cracks
215 and consequently increased the free volumes within the bars that could be filled by the surrounding solution.
216 It can be finally observed that, for all temperatures, specimens exposed to alkali solution showed slightly
217 higher moisture uptake than those exposed to tap water as the former contains more free hydroxide ions (OH^-
218), which work as a solvent for the polymer, thus promoting the solution ingress.

219 **4.2 Chemical and physical degradation of GFRP bars in wet environments**

220 **4.2.1 Effects on Matrix**

221 The effect of the different conditioning environments, temperatures and applied stress levels, on the GFRP
222 matrix was studied at different depths of the samples. In particular, the external surface was analysed using
223 both SEM images and FTIR. FTIR was also employed to examine an inner portion of the bars, yet still
224 sufficiently close to the surface, while the core of the samples was analysed using DMA.
225 FTIR was employed to detect possible chemical changes in the polymeric chain after conditioning. Intensity
226 changes in the hydroxyl group (OH) (Eq. 1) and in the stretching bands of $\text{C}=\text{O}$ and $\text{C}-\text{O}$ were investigated to
227 verify that hydrolysis and oxidation reactions took place. Since the intensity of a FTIR spectrum can be
228 affected by several parameters, it is customary [19] to quantify the changes in a given band as a ratio with the
229 variations of the aromatic group CH , which is very stable and does not easily break apart and react with other
230 substances. Thus, changes in the OH/CH (I3400/I3026) and $\text{C}=\text{O}/\text{CH}$ (I1722/I3026) ratios as well as in the
231 $\text{C}-\text{O}/\text{CH}$ (I1295/I3026) ratio can be used to gage hydrolysis and oxidation reactions, respectively. Similarly,
232 changes in the $\text{C}=\text{C}$ peak, also referred to as curing index [35], were monitored to gain information on the
233 curing process.
234 The FTIR spectra were calculated on the surface of control (REF), unstressed (W and K) and stressed (W-S3
235 and K-S3) samples (**Fig. 7-a**) as well as on a deeper portion of control (REF) and unstressed (W and K)
236 samples (**Fig. 7-b**, grinded samples). All samples were conditioned for 8760 hr at 60°C.



237
 238 **Fig. 7.** FTIR spectra for the resin matrix on (a) the surface of GFRP bars and on (b) grinded samples. Results for
 239 unstressed and stressed (S3) specimens conditioned in water (W) and alkali solution (K) at 60°C for 8760 hr are
 240 compared to benchmark samples (REF).
 241

242 The results of the FTIR analysis on the surface of the samples (Table 3) showed that all the OH/CH ratios
 243 increased with respect to REF and that such increase was more marked in unstressed samples than in stressed
 244 ones. This directly confirms that moisture entered the polymer matrix promoting the hydrolysis reaction and
 245 it also implies that stressed samples had lower chemical interaction (i.e., lower hydrolysis). As the intensity
 246 of OH was similar for unstressed samples (only slightly lower for K), the C=O/CH (I1722/I3026) ratio was
 247 used as an additional indicator of the hydrolysis reaction taking place and to assess the effect of the
 248 conditioning environment. The reduction in C=O/CH (I1722/I3026) was due to the breakage of the end of
 249 the vinyl ester chain and, as suggested by the lower value, the alkaline solution seemed to cause more
 250 breakage of the ester chain than water (i.e. more hydrolysis). Conversely, while oxidation occurred in all
 251 samples as all the C-O/CH (I1295/I3026) ratios increased with respect to REF, this reaction was more
 252 evident in stressed samples than unstressed ones and in water rather than alkaline solution.

253
 254 **Table 3** Band ratios results for FTIR analysis on the outer surface of the samples aged at 60°C for 8760 hours.

Samples	OH/C-H (I3400/3026)		C=O/C-H (I1722/I3026)		C-O/C-H (I1295/I3026)		C=C/C-H (I920/I3026)		C=C/C-H (I1608/I3026)	
	(1)	(2)	(3)	(4)	(5)	(6)	(7)	(8)	(9)	(10)
	Value	(%)	Value	(%)	Value	(%)	Value	(%)	Value	(%)
REF	1.05	-	2.07	-	1.79	-	1.49	-	3.45	-
W	1.40	1.33	1.82	0.88	2.80	1.56	2.47	1.66	2.92	0.85
W-S3	1.16	1.10	2.10	1.01	2.94	1.64	2.73	1.83	3.32	0.96
K	1.32	1.26	1.52	0.73	2.16	1.21	1.98	1.33	2.89	0.84
K-S3	1.16	1.10	2.46	1.19	2.46	1.37	1.87	1.26	3.36	0.97

255
 256 **Error! Reference source not found.** shows that, for all grinded deeper samples, there was a small reduction
 257 of the OH/CH ratio and a negligible variation of the C=O/CH (I1722/I3026) ratio with respect to the REF
 258 samples, suggesting that no hydrolysis reaction occurred in this portion of the bar. The test results also

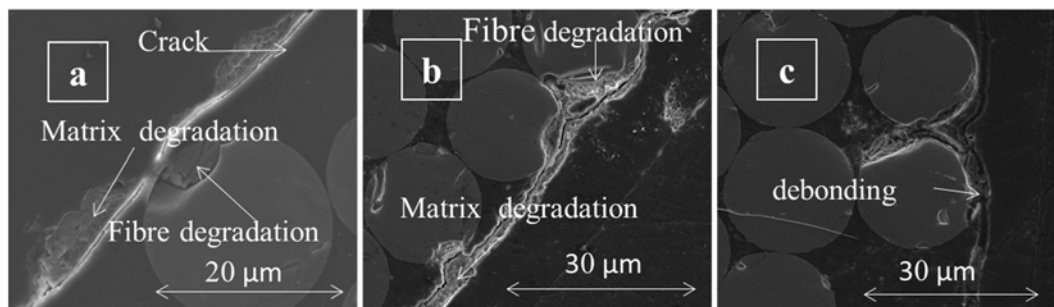
259 showed an increase in the ratio of C-O/CH (I1295/I3026) ratio in both K and W samples due to the oxidation
 260 of the methylene group (CH₂) at the end of the vinyl ester chain.

261 Table 4 Band ratios results for FTIR analysis on a grinded portion of the inner layer of the samples aged at 60°C for 8760
 262 hours.

Samples	OH/C-H (I3400/I3026) (1)		C=O/C-H (I1722/I3026) (2)		C-O/C-H (I1295/I3026) (3)		C=C/C-H (I920/I3026) (4)		C=C/C-H (I1608/I3026) (5)	
	Value	(%)	Value	(%)	Value	(%)	Value	(%)	Value	(%)
	REF	1.17	-	0.57	-	0.70	-	0.79	-	0.62
W	1.13	0.97	0.57	1.00	1.00	1.43	0.98	1.24	1.08	1.74
K	1.13	0.97	0.57	1.00	1.19	1.70	1.11	1.41	1.41	2.27

263
 264 For both surface and grinded specimens, an increase in the C=C/CH (I920/I3026) ratio with respect to REF
 265 was observed (column 4 in Tables 3 and 4). This may be attributed to additional repeating units connecting to
 266 the backbone chain and increasing the number of benzene rings, and consequently the stiffness of the resin.
 267 The ratio of C=C/CH at different locations of the polymer chain (i.e. 1608/I3026) (column 5 in Table 3, 4)
 268 showed a reduction in the outer layer and an increase in the inner part of the bars, thus providing evidence of
 269 degradation on the surface and post curing of the core portion of the bars.
 270 Additional evidence of matrix deterioration (i.e. cracks, voids and de-bonding from the fibres) was provided
 271 by the SEM images of the outer layers of GFRP bars conditioned in water (W) and alkaline solution (K) at
 272 60°C for 8760 hr (Fig. 8).

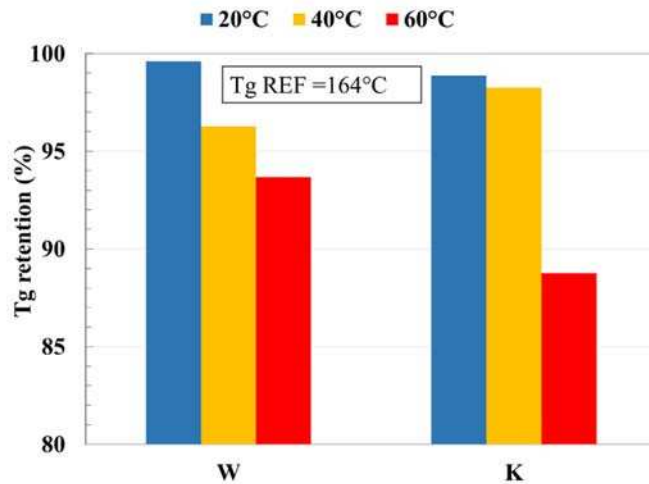
273



274
 275 **Fig. 8.** SEM images of the cross-sections of specimen conditioned in (a) water and (b and c) alkaline solution at 60°C for
 276 8760 hr.

277
 278 The analysis of the innermost part of the GFRP bars was carried out by determining the glass transition
 279 temperature (T_g) of samples obtained from the core of specimens aged for 8760 hr in water (W) and alkaline
 280 solution (K) at 20°C, 40°C and 60°C. After the specimens were removed from the conditioning environment,
 281 they were stored in sealed plastic bags up to the time of testing. The values of T_g were determined according

282 to the storage modulus (E') method. Fig 9 shows that the change in T_g was negligible for low temperatures,
 283 while a reduction of more than 5% was observed at 60°C for both environments. Since a reduction in T_g
 284 indicates a reduction of transfer properties of resin matrix, it can be concluded that, at least at elevated
 285 temperatures, the matrix properties in the core of the specimens were also affected.
 286



287
 288 **Fig. 9.** Change in glass transition temperature (T_g) for the core of specimens conditioned in water (W) and alkaline
 289 solution (K) at different temperatures for 8760 hr.

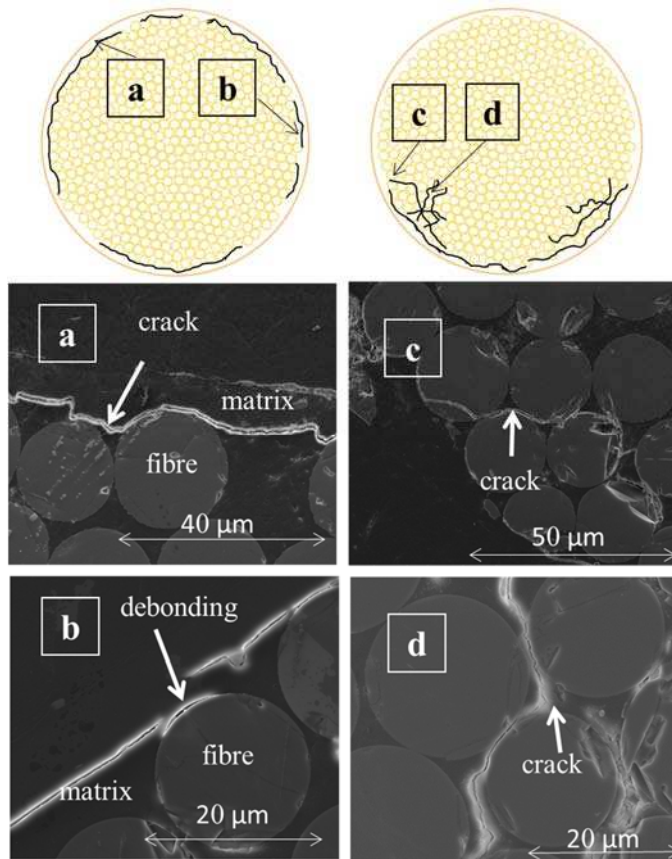
290
 291 All the results confirm that in presence of moisture the higher the conditioning temperatures the higher the
 292 deterioration of the resin matrix and indicate that the polymer chain undergoes disruption (hydrolysis) and
 293 reconstruction (oxidation) of the bond links with possible repercussion on the physical and mechanical
 294 properties of the polymer matrix.

295 4.2.2 Effects on matrix/fibre interface

296 The interface between the matrix and the fibres is a very thin layer (approximately 1 μm) of coupling agent,
 297 consisting of a saline-based material susceptible to moisture and alkaline environments. The assessment of
 298 the deterioration of such a thin layer was only possible by using highly magnified SEM images.

299 **Fig. 10** shows, at the top, the typical crack pattern observed in the cross-section of unstressed (left) and
 300 stressed (right) samples, as well as the approximate locations where the SEM images (a, b, c and d) were
 301 taken. As no significant deterioration was seen in samples conditioned at low temperatures, only images of
 302 samples conditioned in water and alkaline solution at 60°C for 8760 hr are presented. These results confirm
 303 that moisture dissolved the saline substances at the interface causing local loss of bond between fibres and
 304 matrix (i.e., cracks and debonding). In addition, it can be noticed that for the unstressed sample the cracks

305 tend to propagate circumferentially around the outermost layer of fibres, while the cracks are concentrated on
306 the tension side of the stressed samples and propagate both radially and circumferentially as a result of the
307 three-point bending setup used to stress the specimens (**Fig. 3-b**).
308



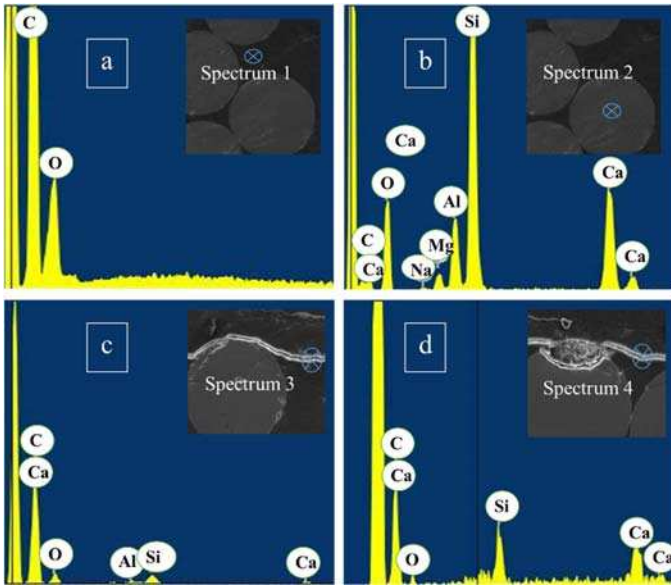
309 **Fig. 10.** SEM images of the cross sections of unstressed specimen (left) and stressed specimens (right) conditioned in
310 water at 60°C for 8760 hr.
311
312

313 4.2.3 Effects on glass fibres

314 Highly magnified SEM images were used to study the degradation of the glass fibres in water and alkaline
315 solution (Eq. 2 and Eq. 3). In addition, as silica (Si), aluminium (Al) and calcium (Ca) are not chemical
316 elements present in a vinyl ester matrix, a precise elemental analysis using EDX was carried out to detect the
317 presence of such elements as a result of the glass fibres dissolution.

318 The results of the EDX analysis carried out on the matrix and the fibres of a reference sample (**Fig 11-a** and
319 **Fig 11-b**, respectively) and on the matrix of samples conditioned in water and alkaline solution at 60°C for
320 8760 hr (**Fig 11-c** and **Fig 11-d**, respectively) are presented in the form of the spectra displaying the
321 concentration (peaks) of each chemical element identified in the analysis.

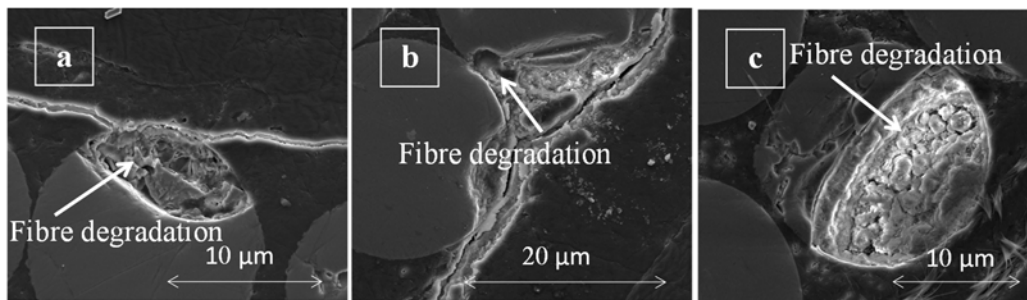
322



323
 324 **Fig. 11.** Results of EDX scans for specimens conditioned (c) in water and (d) alkaline solution at 60°C for 8760 hr are
 325 compared to benchmark samples for (a) matrix and (b) fibres.
 326

327 In all figures, the location where the analysis was performed is indicated by a target. The EDX analysis
 328 detected the aforementioned chemical elements in the resin matrix near to the fibre/matrix interface both for
 329 specimens conditioned in water (W, **Fig 11-c**) and alkaline solution (K, **Fig 11-d**). This confirmed that water
 330 molecules and hydroxide ions, through micro-cracks in the matrix, reached the glass fibres deteriorating
 331 them. Additional evidence of the fibre deterioration within the outer layer was provided by SEM images as
 332 shown in **Fig. 12**.

333



334
 335 **Fig. 12.** SEM images showing the degradation in glass fibres after conditioning in alkaline solution at 60°C for 8760 hr
 336

337 4.3 Mechanical degradation of GFRP bars in wet environments under sustained stress

338 4.3.1 Tensile properties

339 The results of the tensile tests are summarized in Table 5, including average (Avg) tensile strength and
 340 modulus of elasticity, their coefficients of variation (COV) and their retention calculated as percentage of
 341 results for REF. The tensile strength was calculated using a nominal diameter of 8 mm while the modulus of

342 elasticity was calculated as the slope of the stress-strain curve between 20% and 60% of the ultimate tensile
 343 strength.

344 Table 5 Tensile test results

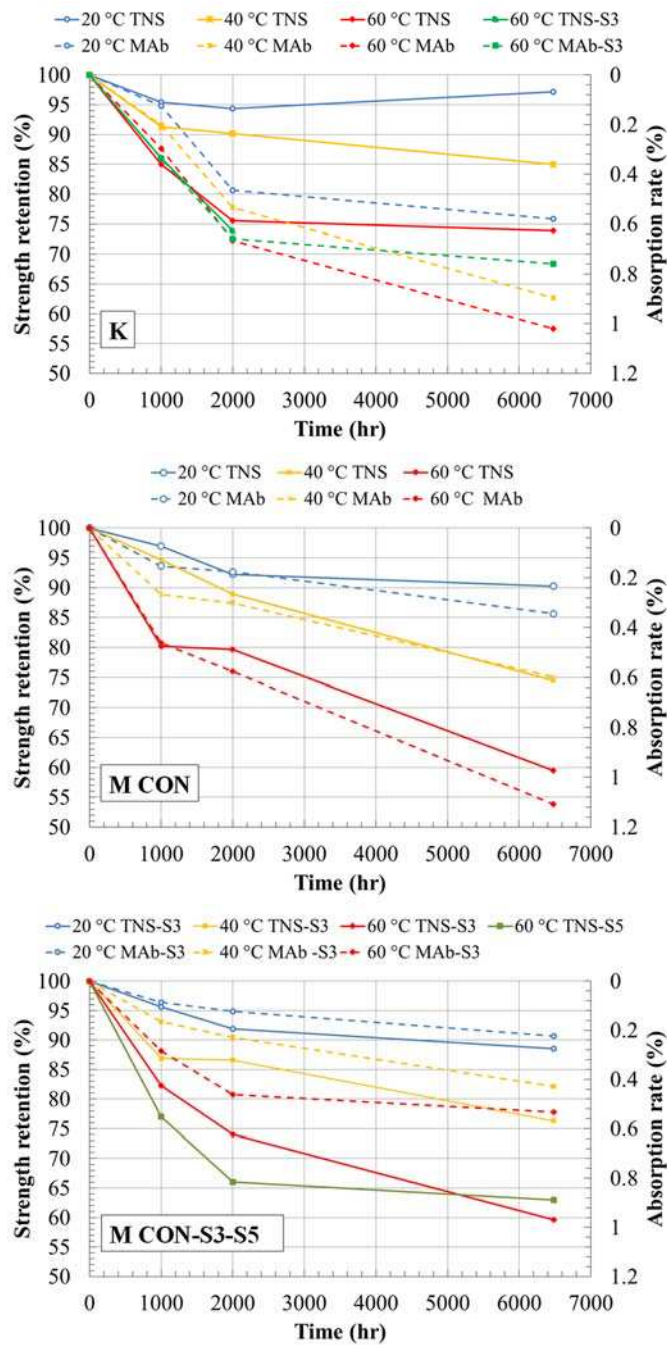
Exposures	Conditioning		Tensile Strength			Modulus of Elasticity		
	Temp (°C)	Time (hr)	Avg (MPa)	COV (%)	Retention (%)	Avg (GPa)	COV (%)	Retention (%)
REF	20	0	1542	1.8	100	56.1	2.7	100
K	20	1000	1472	0.3	95	56.7	0.7	101
	20	2000	1454	0.2	94	53.6	0.6	96
	20	6480	1498	n.a.*	97	58.5	n.a.*	104
	40	1000	1407	1.9	91	57.5	4.0	102
	40	2000	1390	1.3	90	57.0	4.5	102
	40	6480	1310	n.a.*	84	60.4	n.a.*	108
	60	1000	1310	3.1	84	59.2	6.2	106
	60	2000	1139	11.6	73	58.0	1.7	103
	60	6480	997	n.a.*	64	66.4	n.a.*	118
	K-S3	60	1000	1327	5.4	86	58.9	4.4
60		2000	1164	4.5	75	56.1	4.2	100
CON	20	6480	1540	0.7	100	56.7	6.4	101
M-CON	20	2000	1421	5.3	92	55.3	3.4	99
	20	6480	1392	6.9	90	55.5	3.5	99
	40	1000	1458	1.4	95	56.5	0.1	101
	40	2000	1370	1.0	89	57.5	1.9	102
	40	6480	1148	18.0	74	58.4	5.4	104
	60	1000	1244	5.9	80	59.8	6.0	107
	60	2000	1227	1.1	79	58.8	4.2	105
	60	6480	917	1.4	59	55.4	1.9	99
M-CON-S3	20	1000	1473	0.2	96	57.6	1.0	103
	20	2000	1416	1.8	92	61.6	6.5	110
	20	6480	1365	11.5	89	55.5	3.0	99
	40	1000	1228	17.0	87	58.5	0.3	104
	40	2000	1335	3.6	87	57.0	4.2	102
	40	6480	1177	3.6	76	57.2	2.7	102
	60	1000	1233	2.4	82	58.3	2.8	104
	60	2000	1073	11.0	74	58.8	2.7	105
	60	6480	919	4.2	59	61.1	3.4	109
	M-CON-S5	60	1000	1190	14.0	77	59.4	2.2
60		2000	1023	0.6	66	59.9	0.9	107
60		6480	971	4.8	63	58.3	5.0	104

* COV not available since only one specimen was tested.

345

346 **Fig. 13** shows the tensile strength and moisture absorption rate over the conditioning time for unstressed and
 347 stressed specimens exposed to moist concrete (M-CON, M-CON-S3, and M-CON-S5) and alkaline solution

348 (K and K-S3) at 20, 40 and 60°C. The results indicate that tensile strength decreased as moisture uptake
 349 increased and these effects were accelerated by increasing the temperature. It should be mentioned that
 350 moisture absorption and strength retention were measured on different specimens configurations (see Fig. 3)
 351 and the different stress distribution within the direct tension specimens might have affected moisture
 352 absorption, which was possibly underestimated as a result of the different induced cracking pattern.
 353



354 **Fig. 13.** Tensile strength (TNS) retention and moisture absorption (MAb) over time for unstressed and stressed (S3 and
 355 S5) bars conditioned in alkaline solution (K) and concrete (M-CON).
 356
 357

358 The reduction in tensile properties of GFRP bars can be interpreted in light of the results obtained by FTIR
359 and SEM/EDX. The deterioration of the matrix allowed the ingress of hydroxide ions with a two-fold effect:
360 1) causing de-bonding between fibres and matrix, consequently reducing the GFRP ability to transfer
361 effectively the load from the matrix to the fibres; 2) dissolving the glass fibres, thus resulting in a local
362 reduction of the number of fibres effectively contributing to carry the load.

363 In addition, even if the test results showed that the changes in the average tensile modulus of elasticity of
364 most conditioned specimens is negligible, as it varied within the variability of the experimental data, a
365 general increasing trend can be noticed. This beneficial effect on the stiffness was particularly evident in
366 specimens directly exposed to alkaline solution (K) for an extended period of time (6480 hr), showing that
367 the higher the temperature the higher the modulus of elasticity. This could be interpreted as post-curing of
368 the matrix, phenomenon that was also previously captured by FTIR analysis in the inner layers of the bar. In
369 addition, and as supported by the analysis of the SEM micrographs, only a small portion of the bar was
370 subjected to a significant level of deterioration after exposure to the conditioning environments. The majority
371 of the tensile strength reduction occurred within the first 2000 hr for all environments, with a slightly higher
372 degradation rate being observed for the specimens conditioned in alkaline solution (K). The unstressed
373 specimens embedded in concrete (M-CON), exhibited a slightly higher retention rate up to 2000 hr but their
374 strength at 6480 hr was overall lower than that of specimens immersed in alkaline solution. This can be
375 attributed to the formation of salt barriers on the surface of the K specimens that inhibited further diffusion
376 and damage to the microstructure. The application of a sustained stress during conditioning, equivalent to
377 3000 $\mu\epsilon$ and 5000 $\mu\epsilon$, affected slightly only the tensile strength, possibly because the level of imposed strain
378 was small compared to the ultimate strain of the REF samples (i.e. 27000 $\mu\epsilon$).

379 4.3.2 Flexural properties and inter-laminar shear strength

380 **Error! Reference source not found.** summarizes the results of flexural (flexural strength and modulus of
381 elasticity) and inter-laminar shear tests (ILSS) in terms of average values, coefficients of variation and
382 retention for unstressed and stressed bars directly exposed to water (W and W-S3) and alkaline solution (K
383 and K-S3) at 20, 40 and 60°C for 6480 hr.

384 Table 6. The results of flexural (flexural strength and modulus of elasticity) and inter-laminar shear tests (ILSS)

Exp.	Conditioning		Flexural Strength			Modulus of Elasticity			ILSS		
	T (°C)		Avg (MPa)	COV (%)	Retention (%)	Avg (GPa)	COV (%)	Retention (%)	Avg (MPa)	COV (%)	Retention (%)
REF	20		1368	7.1	100	55.6	1.5	100	73	2.5	100

W	20	1360	4.0	99	59.5	1.3	107	66	4.8	90
	40	1326	4.3	97	62.4	0.7	112	63	3.3	86
	60	1124	4.0	82	56.2	1.0	101	55	5.4	75
W-S3	20	1331	6.6	97	56.1	1.7	101	65	3.8	89
	40	1054	8.2	77	65.4	4.6	115	64	3.7	87
	60	1054	5.0	77	58.2	2.7	104	63	4.0	86
K	20	1203	1.6	88	57.8	0.2	103	70	1.6	95
	40	1296	3.5	94	57.9	0.3	103	68	3.5	93
	60	1143	4.0	83	55.8	0.2	100	54	4.0	74
K-S3	20	1306	7.9	95	55.8	2.2	100	66	6.2	90
	40	1157	3.9	84	57.4	2.3	103	64	1.7	87
	60	1145	2.2	83	52.92	2.2	95	61	1.3	85

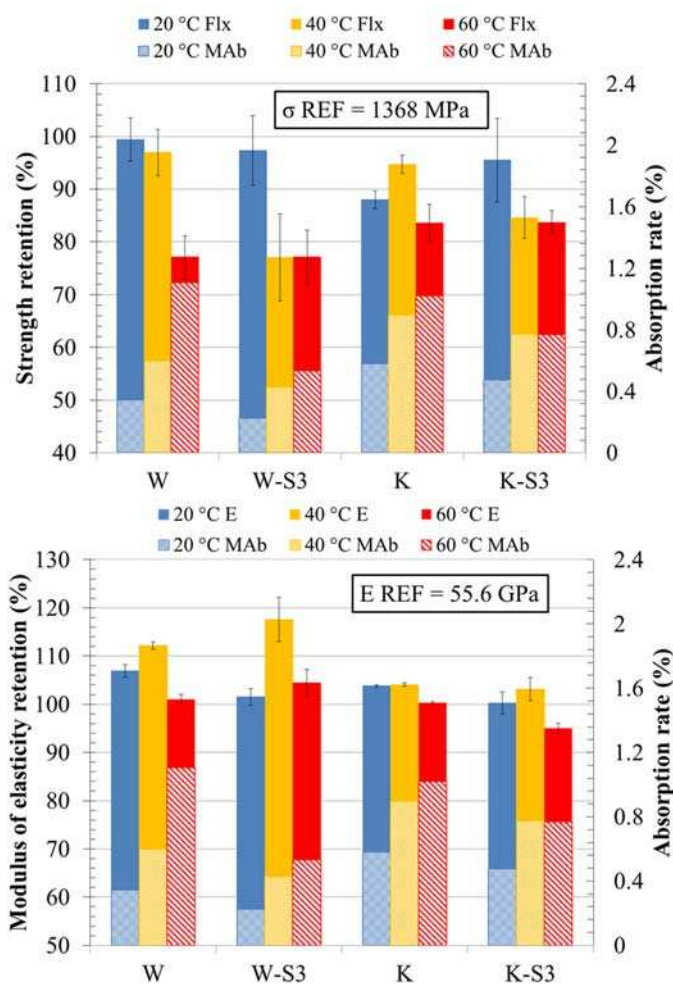
385

386 The retention of mechanical properties is also shown in **Fig. 14** and **Fig. 15** along with the moisture

387 absorption (MAb) rate results to illustrate the effects of moisture ingress on flexural and inter-laminar

388 properties.

389



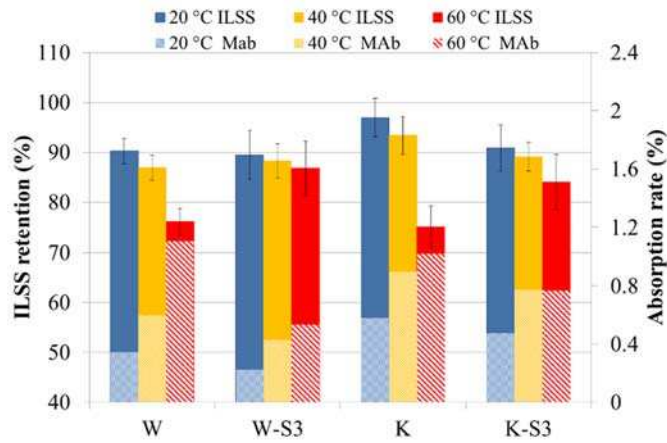
390

391

392

Fig. 14. Flexural strength (Flx) and modulus of elasticity (E) are compared to moisture absorption results (MAb) for different conditioning environments after 6480 hr.

393



394
395
396
397

Fig. 15. Inter laminar shear strength retention (ILSS) is compared to moisture absorption results (MAB) for different conditioning environments after 6480 hr

398
399
400
401
402
403
404
405
406
407
408
409
410
411
412
413
414
415
416

It can be noticed that the average flexural strength of all conditioned specimens decreased compared to the reference specimens. In particular, for exposures at 20 and 60°C, the higher the temperature, the lower the flexural strength, which is in line with the findings previously discussed for TNS and MAb tests. Conversely, at 40°C, the application of sustained stress appears to affect strength retention significantly, as the strength of stressed samples was much lower than that of unstressed ones. However, this behaviour was only recorded for flexural tests and the same trend was not observed in TNS and ILSS tests results. This can be attributed to the different state of stress and failure mode generated within specimens subjected to different test configurations. Although flexural tests are relatively simple to perform, the different behaviour of composite materials in tension and compression (with unidirectional FRP being typically characterised by a lower compressive strength) can result in underestimating tensile strength and in an increased variability of results. The variability in the results obtained from flexural tests can also increase for conditioned specimens, especially when deterioration occurs at the fibre/matrix interface and can affect compression behaviour. As stiffness is always determined within the perfectly elastic load-deformation range, the values determine for flexural stiffness generally agree well with those obtained from direct tension tests. The average values of the flexural modulus of elasticity increased marginally for most of the specimens, with the exception of samples conditioned in water at 40°C for which the flexural stiffness increased more than 10%. The overall higher stiffness could have been caused by post-curing of the matrix during conditioning. This is in line with the results obtained from the direct tension tests as well as the FTIR findings, albeit at lower temperature.

417 The results from the ILSS tests show that the higher the conditioning temperature, the higher the strength
418 degradation, but also that stressed specimens experienced lower reduction in ILSS than unstressed ones.
419 Such findings are in good agreement with previous tests carried out in this study, suggesting that the
420 increased temperature favoured the ingress of moisture leading to a premature inter-laminar de-bonding and
421 that the state of stress induced using the test setup described in Fig 3b limited moisture ingress mitigating the
422 reduction in ILSS.

423

424 **5 Conclusions**

425 The present study investigated the mechanical performance and physical and chemical characteristics of
426 GFRP bars conditioned in different environments with and without sustained stress. The mechanical and
427 micro structural properties were evaluated by direct tension test, flexural tests, inter-laminar shear tests,
428 moisture absorption, SEM-EDX, FTIR, and DMA. On the basis of the discussion presented above, the
429 following conclusions can be drawn:

430 1) Moisture uptake of the tested GFRP bars occurred at a faster rate up to 4600 hr. The different rate of
431 diffusion can be attributed to the moisture absorption via capillaries and micro-cracks in the resin matrix.
432 This mechanism continues until moisture reaches the fibres, which provide a barrier and restrict moisture
433 flow. The tests results also confirmed that diffusion rate during the initial stages is highly dependent on the
434 temperature, and higher temperatures lead to higher absorption rates. However, the specimens exposed to
435 alkaline solution showed slightly higher moisture uptake than those exposed to tap water as the former
436 contains more free hydroxide ions (OH⁻), which work as a solvent for the polymer, thus promoting ingress of
437 the solution.

438 2) For temperature up to 40°C the degradation observed in specimens exposed to K and M-CON
439 environments were similar, whereas for higher temperatures and after 2000hr of exposure less degradation
440 was observed in specimens exposed to K environment. This can be attributed to deposition of salts on the
441 bars surface, which provided a barrier and restricted moisture diffusion into the bars, thus potentially leading
442 to underestimate strength retention.

443 3) Unexpectedly, the stressed specimens exhibited lower absorption rate than the unstressed counterparts.
444 This may be attributed to the method that was used to induce the desired strain (i.e. imposing the required
445 curvature via elastic bending) and the closing of micro cracks within the compression zone of the specimens.

446 Further tests on bars subjected to different stress distributions (e.g. uniform tension) should be carried out to
447 examine this aspect in more details.

448 4) The tensile test results clearly show that the tensile strength of the tested GFRP bars was affected by the
449 conditioning environments. In general, higher temperatures and higher levels of sustained stress lead to
450 higher strength degradation. Similar trends were observed for all types of exposure with most of the tensile
451 strength reduction occurring within the first 2000 hr. This can be attributed to the high diffusion of water
452 molecules through the resin matrix outer layer inducing damage to the fibre/resin interface. After 2000 hr
453 exposure, bars embedded in concrete under sustained stress equivalent to 5000 $\mu\epsilon$ conditioned in water at
454 60°C exhibited the higher reduction in strength due to the acceleration of moisture uptake caused by the high
455 temperature and as a result of the higher level of damage in the matrix caused by the sustained stress.

456 5) The reduction in the tensile strength of all conditioned samples subjected to a sustained stress equivalent
457 to 3000 $\mu\epsilon$ was within the limits recommended in the Canadian code for high durability bars [21]. A lower
458 average strength retention was observed only for the specimens subjected to the higher sustained stress
459 equivalent to 5000 $\mu\epsilon$.

460 6) No significant change was observed in the elastic modulus of the tested GFRP bars regardless of the
461 conditioning environment or exposure period. Although a small degree of degradation was observed through
462 SEM and EDX in the outer resin matrix layer and some of the glass fibres closer to the surface of the bar, the
463 observed level of damage was too small to result into an appreciable stiffness reduction. Some of the samples
464 exhibited a slight enhancement in stiffness, possibly due to the post curing of the resin matrix, as confirmed
465 by FTIR results.

466 7) The change in flexural properties (e.g. strength, stiffness) was in line with what observed as a result of
467 direct tension tests.

468 8) No significant fibre deterioration was observed through SEM/EDX within the cross-section of the bars,
469 with the majority of the damage being limited to a small percentage of glass fibres within the outer surface
470 layer. Microstructural changes in the matrix and debonding between fibre/matrix seem to be the main issues
471 affecting the long term mechanical properties of the tested GFRP bars.

472 9) The EDX scan detected additional elements such as silicon (Si), aluminium (Al), and calcium (Ca) in the
473 interface zone and in the resin matrix. This is attributable to the dissolution of the fibres and leaching of their
474 components into the resin matrix.

475 10) The FTIR analysis showed a significant increase in the amount of hydroxyl groups at the surface of the
476 material. This is an indication of chemical degradation in the resin matrix.
477 In summary, the long term mechanical properties of GFRP bars appear to be mainly affected by diffusion of
478 moisture through the resin rich layer and the debonding between the fibre/matrix interfaces due to the
479 dissolution of the silane coupling agents. Therefore, more developmental work could focus on these aspects
480 to improve further the durability of GFRP bars for civil engineering application. It should be noted that the
481 above conclusions are based on the characterization of a specific bar with a given glass fibre/resin
482 combination and may not directly extend to other types of FRP rebars. Additional tests should be performed
483 on GFRP bars with different types of resin matrixes to provide statistically significant results and
484 conclusions.

485 **6 Funding**

486 This work is financially supported by The University of Benghazi

487 **7 Acknowledgments**

488 The authors gratefully acknowledge the assistance of the technical staff of the Heavy Structure Laboratory of
489 the University of Sheffield and Dr Maria Criado for her professional guidance in performing the
490 microstructural characterisation.

491 **8 References**

- 492 1. Nkurunziza G, Debaiky A, Cousin P, Benmokrane B. Durability of GFRP bars: A critical
493 review of the literature. *Progress in Structural Engineering and Materials*, 2005; 7(4):194-209.
- 494 2. Dejke V. Durability of FRP Reinforcement in Concrete. Literature and Experiments. Sweden:
495 Department of Building Materials. Chalmers University of Technology Goteborg, 2001, p. 210.
- 496 3. Karbhari V, Chin W, Hunston D, Benmokrane B, Juska T, Morgan R, Lesko J, Sorathia U,
497 Reynaud D. Durability gap analysis for fiber-reinforced polymer composites in civil
498 infrastructure. *Journal of composites for construction*, 2003; 7(3):238-247.
- 499 4. Micelli F, Nanni A. Durability of FRP rods for concrete structures. *Construction and Building*
500 *materials*, 2004; 18(7): 491-503.
- 501 5. Benmokrane B, Wang P, Ton-That TM. Durability of glass fiber-reinforced polymer
502 reinforcing bars in concrete environment. *J Compos Constr*, 2002; 6(3):143–153.
- 503 6. Chen Y, Davalos J, Ray I, Kim H. Accelerated aging tests for evaluations of durability
504 performance of FRP reinforcing bars for concrete structures. *Composite Structures*, 2007.
505 78(1):101-111.
- 506 7. Nelson WB. Accelerated testing: statistical models, test plans, and data analysis. John Wiley &
507 Sons; 2009.

- 508 8. Bank LC, Gentry TR, Barkatt A. Accelerated Test Methods to Determine the Long-Term
509 Behavior of FRP Composite Structures: Environmental Effects. *Journal of Reinforced Plastics*
510 *and Composites*, 1995; 14(6):559-587.
- 511 9. Byars E, Waldron P, DeJke V, Demis S, Heddadin S. Durability of FRP in concrete
512 deterioration mechanisms. *International Journal of Materials and Product Technology*, 2003;
513 19(1):28-39
- 514 10. Benmokrane B, Elgabbas F, Ehab A, ASCE M and Cousin P. Characterization and comparative
515 durability study of glass/vinylester, basalt/vinylester, and basalt/epoxy FRP bars. *Journal of*
516 *Composites for Construction*, 2015; 19(6):04015008.
- 517 11. Mufti AA, Onofrei M, Benmokrane B, Banthia N, Boulfiza M, Newhook J, Bakht B, Tadros G,
518 Brett P. Report on the studies of GFRP durability in concrete from field demonstration
519 structures. In: *Proceedings of the Conference on Composites in Construction*. Lyon, Jul, 2005.
520 p.11-13
- 521 12. Sawpan MA, Mamun AA, Holdsworth PG. Long term durability of pultruded polymer
522 composite rebar in concrete environment. *Materials & Design*, 2014; 57:616-624
- 523 13. Robert M, Benmokrane B. Behavior of GFRP reinforcing bars subjected to extreme
524 temperatures. *Journal of Composites for Construction*, 2009; 14(4):353-60.
- 525 14. Bank LC, Gentry TR, Barkatt A, Prian L, Wang F, Mangla SR. Accelerated aging of pultruded
526 glass/vinylester rods. In: *Second International Conference on Composites in Infrastructure*,
527 Januaray, 1998 (Vol. 2).
- 528 15. Robert M, Benmokrane B. Combined effects of saline solution and moist concrete on long-term
529 durability of GFRP reinforcing bars. *Construction and Building Materials*, 2013; 38:274-84.
- 530 16. Fergani H, Di Benedetti M, Guadagnini M, Lynsdale C, Mais C. Long term performance of
531 GFRP bars under the combined effects of sustained load and severe environments. In: *The 8th*
532 *International Conference on Fibre-Reinforced Polymer (FRP) Composites in Civil Engineering*.
533 Hong Kong, 2016.
- 534 17. Serbescu A, Guadagnini M, Pilakoutas K. Mechanical characterization of basalt FRP rebars and
535 long-term strength predictive model. *Journal of Composites for Construction*. 2014;
536 19(2):04014037.
- 537 18. Robert M, Cousin P, Benmokrane B. Durability of GFRP reinforcing bars embedded in moist
538 concrete. *Journal of Composites for Construction*. 2009; 13(2):66-73.
- 539 19. Kamal AS, Boulfiza M. Durability of GFRP rebars in simulated concrete solutions under
540 accelerated aging conditions. *Journal of Composites for Construction*. 2010; 15(4):473-81.
- 541 20. fib Task-group 9.3. FRP Reinforcement in RC Structures. *fib Bulletin*. 2007; 40, (147).
- 542 21. Canadian Standard Association (CSA). Specification for fibre-reinforced polymers. CAN/CSA
543 S807-10. Rexdale, Ontario, Canada; 2010. p 27.
- 544 22. ACI 440.3R-04. Guide test methods for fiber-reinforced polymers (FRPs) for reinforcing or
545 strengthening concrete structures, ACI Committee 440, American Concrete Institute,
546 Farmington Hills, Michigan, USA; 2004.

- 547 23. Almusallam TH, Al-Salloum YA. Durability of GFRP rebars in concrete beams under
548 sustained loads at severe environments. *Journal of composite materials*, 2006; 40(7):623-37.
- 549 24. Wu G, Dong ZQ, Wang X, Zhu Y, Wu ZS. Prediction of long-term performance and durability
550 of BFRP bars under the combined effect of sustained load and corrosive solutions. *Journal of*
551 *Composites for Construction*, 2014; 19(3):04014058.
- 552 25. Nkurunziza, G, Benmokrane B, Debaiky A, Masmoudi R, Effect of sustained load and
553 environment on long-term tensile properties of glass fiber-reinforced polymer reinforcing bars.
554 *ACI structural journal*, 2005. 102(4):615.
- 555 26. Wang J, GangaRao H, Liang R, Zhou D, Liu W, Fang Y. Durability of glass fiber-reinforced
556 polymer composites under the combined effects of moisture and sustained loads. *Journal of*
557 *Reinforced Plastics and Composites*, 2015; 21:1739-54.
- 558 27. Bakis CE. Durability of GFRP reinforcement bars. In *Advances in FRP Composites in Civil*
559 *Engineering*. Berlin:Springer, 2011. p.33-36.
- 560 28. Broomfield, PJ. *Corrosion of Steel in Concrete: Understanding, Investigation and Repair*.
561 London: Chapman & Hall, 1997. p.1-215.
- 562 29. Mias C, Guadagnini M, Torres L, Fergani H. Strength of GFRP RC beams after sustained
563 loading. In: *Proceedings of FRPRCS-12 & APFIS-15.Conference.Nanjing*, 2015.
- 564 30. ASTM Standard D4475,2002(2016), "Test Method for Apparent Horizontal Shear Strength of
565 Pultruded Reinforced Plastic Rods By the Short-Beam Method". ASTM International, West
566 Conshohocken, PA.
- 567 31. ASTM Standard D 4476, 2003(2014), "Test Method for Flexural Properties of Fiber Reinforced
568 Pultruded Plastic Rods,". ASTM International. West Conshohocken, PA.
- 569 32. ASTM Standard D7028,2007(2015),"Test Method for Glass Transition Temperature (DMA
570 Tg) of Polymer Matrix Composites by Dynamic Mechanical Analysis (DMA) ", ASTM
571 International. West Conshohocken, PA.
- 572 33. ASTM Standard D570,1998(2010), "Test Method for Water Absorption of Plastics, ", ASTM
573 International. West Conshohocken, PA.
- 574 34. Lu Z, Xian G, Li H. Effects of exposure to elevated temperatures and subsequent immersion in
575 water or alkaline solution on the mechanical properties of pultruded BFRP plates. *Composites*
576 *Part B: Engineering*, 2015; 77:421-430.
- 577 35. Mousa A, Karger-Kocsis J. Cure characteristics of a vinyl ester resin as assessed by FTIR and
578 DSC techniques. *Polymer and Polymer Composites*. 2000 Jan 1;8(7):455-60.